bioRxiv preprint doi: https://doi.org/10.1101/675413; this version posted June 20, 2019. The copyright holder for this preprint (which was not certified by peer review) is the author/funder. All rights reserved. No reuse allowed without permission.

Floral signals evolve in a predictable way under artificial and pollinator selection in *Brassica rapa* using a G-matrix

Pengjuan Zu[1, 2*], Florian P. Schiestl[1], Daniel Gervasi[1], Xin Li[3], Daniel Runcie[3], Frédéric Guillaume[4]

[1]Department of Systematic and Evolutionary Botany, University of Zürich, Zollikerstrasse 107, CH-8008 Zürich, Switzerland

[2] Department of Civil and Environmental Engineering, Massachusetts Institute of Technology, 77 Massachusetts Avenue, 02139 Cambridge, MA, USA

[3]Department of Plant Sciences, University of California Davis, One Shields Avenue, Davis, CA 95616, USA

[4]Department of Evolutionary Biology and Environmental Studies, University of Zürich, Winterthurerstrasse 190, CH-8057 Zürich, Switzerland

*author for correspondence

pzu@mit.edu

bioRxiv preprint doi: https://doi.org/10.1101/675413; this version posted June 20, 2019. The copyright holder for this preprint (which was not certified by peer review) is the author/funder. All rights reserved. No reuse allowed without permission.

Abstract

Background

Angiosperms employ an astonishing variety of visual and olfactory floral signals that are generally thought to evolve under natural selection. Mathematical tools for predicting multiple traits have been developed for decades and have advanced our understanding of evolution in various biological systems. Nevertheless, very few studies have yet attempted to predict the evolutionary trajectories of floral traits, particularly when considering a comprehensive set of genetically correlated floral traits.

Results

We used data from an artificial and a pollinator (bumblebee, hoverfly) selection experiment with fast cycling *Brassica rapa* plants to predict evolutionary changes of 12 floral volatiles and 4 morphological floral traits in response to selection. Using the observed selection gradients and the genetic variance-covariance matrix (G-matrix) of the traits, we showed that the responses of most floral traits including volatiles were predicted well in artificial- and bumblebee-selection experiment. Genetic covariance had a mixed of constrained and facilitated effects on evolutionary responses. We further revealed that G-matrix also evolved in the selection processes. Nevertheless, the ancestral G-matrix can still be used for predicting micro-evolutionary scenarios.

Conclusions

Overall, our integrative study shows that floral signals, and especially volatiles, evolve under selection in a mostly predictable way, at least during short term evolution. Evolutionary constraints stemming from genetic covariance affected traits evolutionary trajectories and thus it is important to include genetic covariance for predicting the evolutionary changes of a comprehensive suite of traits. Other processes such as resource limitation and selfing also needs to be considered for a better understanding of floral trait evolution.

Key words: adaptive evolution, artificial selection, *Brassica rapa*, experimental evolution, floral scent, G-matrix, multivariate prediction, pollinator selection.

bioRxiv preprint doi: https://doi.org/10.1101/675413; this version posted June 20, 2019. The copyright holder for this preprint (which was not certified by peer review) is the author/funder. All rights reserved. No reuse allowed without permission.

Introduction

Flowers are complex organs with enormous diversity in morphology, color and scent. These visual and olfactory components, which characterize the radiation of angiosperms, are recognized to evolve as a means of interaction with their biotic environment (Schiestl & Johnson, 2013; Leonard & Francis, 2017). One important driver, the pollinators, has been emphasized to be important for floral trait evolution since long (Darwin, 1862; Grant, 1949). However, only a handful studies have attempted to test the predicted adaptive evolution of floral traits to pollinator selection (Campbell, 1996; Galen, 1996; Mitchell *et al.*, 1998; Morgan & Ashman, 2003; Caruso, 2004). Moreover, these studies only examined one or a few morphological traits at a time, whereas interactions of flowers with other organisms are typically mediated by a combination of traits of morphological and/or olfactory nature (Raguso & Willis, 2005; Schiestl, 2015). Therefore, a well-designed experiment with multiple traits measurement is required to predict and test the joint evolution of a suite of floral traits under natural or artificial selection.

Mathematically, genetic (co)variance matrix (G-matrix) and phenotypic selection (β) are the two parameters for predicting the evolutionary changes (Δz) of a suite of traits by using multivariate breeder's equation $\Delta z = G^* \beta$ (Lande, 1979; Lande & Arnold, 1983). A great number of empirical studies have documented significant heritability and genetic (co)variance of diverse floral traits (Ashman & Majetic, 2006; Kaczorowski *et al.*, 2008; Zu *et al.*, 2016; Zu & Schiestl, 2017), as well as phenotypic selection acting on them (Gómez, 2003; Irwin & Strauss, 2005; Sandring & Ågren, 2009; Sletvold & Ågren, 2010; Hopkins & Rausher, 2012; Parachnowitsch *et al.*, 2012; Ågren *et al.*, 2013; Gross *et al.*, 2016; Gervasi & Schiestl, 2017). Among those traits, floral scents have rarely been considered. Floral scents are usually highly variable and diverse on all taxonomic levels (Knudsen 2006). We recently showed that this variation has a strong heritable genetic component (20% - 45%, Zu *et al.*, 2016). Together with studies documenting natural selection on scent (Schiestl *et al.*, 2010; Ehrlén *et al.*, 2012; Parachnowitsch *et al.*, 2012; Gross *et al.*, 2016; Gervasi & Schiestl, 2017), this suggests that their evolution can be predicted, although such predictions have never been attempted.

bioRxiv preprint doi: https://doi.org/10.1101/675413; this version posted June 20, 2019. The copyright holder for this preprint (which was not certified by peer review) is the author/funder. All rights reserved. No reuse allowed without permission.

In this study, we predict floral traits evolution and test the predictive power of complex trait evolution using a G-matrix. We used data from two forward-in-time experimental evolution experiments that documented genetic co-variation and evolutionary responses in floral traits of fast cycling *Brassica rapa* plants. The first parameter G of the plant population was estimated from a three-generation bi-directional artificial selection experiment on plant height (Zu & Schiestl, 2017). In that study, tall- and short-plants were selected artificially for building the two directional lines, in addition to a control line built with randomly selected plants. Four morphological floral traits and 12 floral volatiles were measured for each generation. Control lines in this experiment were used to estimate G-matrix. The other parameter β was calculated from four evolutionary scenarios: two from the tall- and short-selection lines in the artificial selection experiment mentioned above (Zu & Schiestl, 2017); the other two from a 9-generation pollinator selection experiment (Gervasi & Schiestl, 2017). The pollinator selection experiment was carried out with bumblebees and hoverflies as the selection agents separately. The same set of floral traits were measured, and the parental plants were from the same seed bank as in the artificial-selection experiment.

In addition to the primary goal of this study to predict and examine floral traits evolution by employing the multivariate breeder's equation, we also tested how the evolutionary trajectory of a trait would be affected (constrained/enhanced) by genetic correlations with traits by dissecting the total responses to selection into direct responses (caused by direct selection on target traits) and indirect responses (caused correlated responses through genetic covariance). Moreover, we assessed the evolution of genetic architectures (G-matrices) throughout the artificial selection processes.

Results

Predictions in the artificial selection experiment

Tall- and short-directional selection can be regarded as the mirrored replicate to each other. The selection gradients of tall and short artificial selection lines were approximately opposite numbers to each other (Table S1), leading to a symmetric pattern of predicted changes of the floral traits: most traits increased in tall line and decreased in short line (Fig. 1). Plant height, the direct and only target of artificial

bioRxiv preprint doi: https://doi.org/10.1101/675413; this version posted June 20, 2019. The copyright holder for this preprint (which was not certified by peer review) is the author/funder. All rights reserved. No reuse allowed without permission.

selection, was predicted accurately in both lines. Flower size traits (PW marginally, PL and FL) were predicted to decrease in short lines and matched the observations, and increase in tall lines, and, however, mismatched the observations (Fig. 1). VOCs were predicted well in most cases (filled violin plots, Fig. 1) in both lines except for three compounds in short lines (empty violin plots, Fig. 1). Note that the amount of some VOCs did not change significantly (red dashed-outlined violins, Fig. 1) although the predictions were correct (filled violins, Fig. 1).

Predictions in the pollinator-selection experiment

In this experiment, selection was stronger in the bumblebee than the hoverfly treatment (Table S2). Consequently, observed and predicted changes were larger in the bumblebee than the hoverfly treatment (Fig. 1, Fig. S1; Table 1). In the bumblebee treatment, our predictions overestimated the evolutionary changes of all morphological traits, while responses of scent compounds (all 12 but benzyl nitrile, BenN) were correctly predicted (Fig. 1; Table 1). Among these seven VOCs significantly increased (solid-outlined violins, Fig. 1), and the other four VOCs were not (dashed-outlined violins, Fig. 1). In the hoverfly treatment, evolutionary responses of only 4 traits were correctly predicted (Fig. 1, Fig. S1; Table 1), among which petal length (PL) was the only one trait that changed significantly (solid-outlined violins).

Effects of genetic covariance on predicting evolutionary trajectories

We separate genetic variance-covariance matrix (**G**) into genetic variance matrix (**G0**) and genetic covariance matrix (**G'**). By comparing evolutionary responses using these three different matrices with the observed changes, we can disentangle the effects of genetic covariance on prediction. In the artificial selection experiment, the only trait under direct selection was height (i.e., **β** has only one non-zero element, see Table S1), and the observed changes in the other traits are thus entirely composed of their indirect responses to the selection on height.

In the bumblebee selection experiment, selection targeted multiple traits with a mixture of positive and negative values (seven positive and nine negative values, Table S2). The direct component of the response predicted from the **G0**-matrix, reflecting the nature of the selection acting on them, showed the same positive or negative responses corresponding to their selection (Table 1). However, the observed responses were positive for all but one trait (MeS) (Table 1). Total predicted

bioRxiv preprint doi: https://doi.org/10.1101/675413; this version posted June 20, 2019. The copyright holder for this preprint (which was not certified by peer review) is the author/funder. All rights reserved. No reuse allowed without permission.

responses (predicted from **G**-matrix) and indirect responses (predicted from **G'**-matrix) were all positive, if not insignificant from zero (Table 1). The opposition between negative selection and positive total response is indicative of strong constraints acting on targets of negative selection. On the other hand, the response to selection was facilitated in the direction of selection when both the direct and indirect components of the response are aligned with the selection gradient, as found for height (Height), phenylacetaldehyde (PAA), methyl salicylate (MeB), and indole (Ind) (Table 1).

The picture was different in the hoverfly treatment with a mix of positive and negative observed trait changes and eight traits with a predicted direct response in the same direction, but no selection gradient significantly different from zero. Phenotypic changes were better predicted without covariance only for petal width and petal length in the bumblebee experiment and flower diameter in the hoverfly experiment (Table 1).

In addition to comparing the effects of genetic covariance on individual traits, we measured the overall constraining effect of genetic co-variation on the response to selection by comparing the angle $\boldsymbol{\theta}$ between the selection response vector ($\Delta\mathbf{z}$) and the first PC of **G** (PC1, or $\boldsymbol{g}_{\max}$) with the angle $\boldsymbol{\gamma}$ between $\Delta\mathbf{z}$ and the selection gradient ($\boldsymbol{\beta}$). In the tall and short artificial selection experiments, the trait responses were strongly aligned with $\boldsymbol{g}_{\max}$, with $\boldsymbol{\theta}$ angle of 12.5 degree (95% HPD: 9.2, 16.6) and 11.2 degree (95% HPD: 7.2, 14.7), respectively. Given the close association of $\boldsymbol{g}_{\max}$ with the first trait axis (height) (Fig. 2c) and thus with the selection gradients under artificial selection, the angle $\boldsymbol{\gamma}$ between $\Delta\mathbf{z}$ and $\boldsymbol{\beta}$ is 9.9 and 8.9 degree in tall and short, respectively, which are within the 95% HPD of $\boldsymbol{\theta}$ in both cases. In contrast, under pollinator selection, $\Delta\mathbf{z}$ is more aligned with $\boldsymbol{g}_{\max}$ than $\boldsymbol{\beta}$, with $\boldsymbol{\theta}$ of 26.9 degree (95% HPD: 22.3, 33) and 60.8 degree (95% HPD: 57.1, 63.5), when compared to $\boldsymbol{\gamma}$, equal to 66.5 and 89.2 degree for bumblebee and hoverfly treatments, respectively.

Evolution of the G-matrix during artificial selection

By examining the G-matrices of the three lines in the artificial selection experiment, we found that a drastic decrease of the additive genetic variance of height in the tall line, with an estimate around 2.8 cm^2, compared to the short line, which remained as high as in the control line around 23 cm^2. This resulted in a large decrease of the

bioRxiv preprint doi: https://doi.org/10.1101/675413; this version posted June 20, 2019. The copyright holder for this preprint (which was not certified by peer review) is the author/funder. All rights reserved. No reuse allowed without permission.

contribution of $\boldsymbol{g}_{max}$ (PC1) of $\mathbf{G}_{tall}$ to the total variance relative to $\mathbf{G}_{control}$ and $\mathbf{G}_{short}$ (see Fig. 2a-b, Table S5). The orientation of $\boldsymbol{g}_{max}$ also changed in $\mathbf{G}_{tall}$, with reduced alignment with the height axis (Fig. 2c). The other eigenvalues and eigenvectors are, however, more constant across lines (Fig. 2a). For instance, the second eigenvector (PC2) is more consistently orthogonal to the height trait axis in the three **G**-matrices (Fig. 2c).

Using the random skewers method, we found strong correlations of the mean selection response among matrices, larger than 70% for all three comparisons, although not significantly so between $\mathbf{G}_{tall}$ and $\mathbf{G}_{short}$, and very strong similarity between $\mathbf{G}_{control}$ and $\mathbf{G}_{short}$ (Table 2). The three G-matrices thus shared a significant portion of their structure. $\mathbf{G}_{control}$ would predict selection responses similar to $\mathbf{G}_{short}$ and to a lesser extent to $\mathbf{G}_{tall}$. Further analysis of the similarity of the size and orientation of the eigenvectors of the G-matrices in the hierarchical analysis confirmed the similarity in shape between $\mathbf{G}_{control}$ and $\mathbf{G}_{short}$ and the dissimilarity of $\mathbf{G}_{tall}$ with $\mathbf{G}_{control}$, and with $\mathbf{G}_{short}$ to a smaller degree (see Table 2). The G-matrix in the tall lines thus evolved more than in the short lines mostly because of the change in the genetic variance of plant height. $\mathbf{G}_{short}$ remained closer to the starting G-matrix ($\mathbf{G}_{control}$) over the course of the experiment.

*Evaluation of the estimation of the **G**-matrices*

Randomization tests of G-matrices were conducted to examine whether G-matrix captured the meaningful biological structures rather than random assembling. The results revealed that $\mathbf{G}_{control}$ was estimated with highest accuracy compared to $\mathbf{G}_{tall}$ and $\mathbf{G}_{short}$. The majority of the genetic covariance elements (101 out of 120) and additive genetic variances (14 out of 16) in $\mathbf{G}_{control}$ were significant at the level of FDR < 0.05, after correcting for multiple testing (false discovery rate: Benjamini & Hochberg 1995). In $\mathbf{G}_{tall}$, 11 variance and 55 covariance elements were significant, and 15 and 72 elements, respectively, in $\mathbf{G}_{short}$ (Table S4), at the same FDR level.

Discussion

Total evolutionary responses are made up of direct and indirect responses. We could predict the evolutionary response of floral traits subject to two types of selection pressures by combining estimates of the ancestral G-matrix of the traits with estimates of the selection gradients acting on them, with relatively high accuracy. Importantly,

bioRxiv preprint doi: https://doi.org/10.1101/675413; this version posted June 20, 2019. The copyright holder for this preprint (which was not certified by peer review) is the author/funder. All rights reserved. No reuse allowed without permission.

we found that predictions based only on the direct trait responses to selection failed to predict the observed responses and that the observed responses were biased towards the line of least genetic resistance ($\boldsymbol{g}_{\max}$) of the G-matrix. This indicates that making correct evolutionary predictions requires the additional knowledge of the indirect trait responses caused by multivariate selection acting on genetically correlated phenotypic traits. The pattern of genetic covariation among traits thus strongly affected the outcome of selection in the artificial and pollinator selection experiments. Although this pattern of trait covariation can change during evolution, we further showed that using an ancestral G-matrix, here estimated in the control lines, can lead to accurate evolutionary predictions over just a few generations. This approach allowed us to better understand how pollinators, the selective agents, interact with the complex set of floral traits composed of floral scent and morphology and may influence their evolution.

We observed a few discrepancies between our evolutionary predictions and observed responses that need to be examined. In particular, the responses of the morphological traits in the artificial selection for tall plants did not show the expected increase of flower size but instead showed a decrease, despite the positive genetic correlations of flower size with plant height (see $\mathbf{G}_{\text{control}}$ in Table S4), which remained positive during selection (see $\mathbf{G}_{\text{tall}}$ in Table S4). It thus cannot be caused by an evolutionary change of the sign of the genetic correlations with height. Instead, this selection experiment may have revealed an underlying resource allocation trade-off masked by the apparent positive genetic covariation between plant height and the size of the reproductive organs. This is reminiscent of classical theory on the effect of variation in resource acquisition and allocation on fitness components (Van Noordwijk & de Jong, 1986; Houle, 1992; Agrawal *et al.*, 2010), which states that a positive correlation between fitness components can be observed despite an underlying trade-off when individuals vary more in the acquisition than in the allocation of their resources. Variation in resource acquisition among the genotypes may have been pre-existing in the base population of *B. rapa*, and lead to the observed positive correlation between traits pertaining to two fitness components, plant reproduction for flower size traits, and plant somatic growth for plant height. However, the observation of a negative correlated response of flower size to selection for reduced plant height in the low artificial selection experiment is more in line with

bioRxiv preprint doi: https://doi.org/10.1101/675413; this version posted June 20, 2019. The copyright holder for this preprint (which was not certified by peer review) is the author/funder. All rights reserved. No reuse allowed without permission.

a positive correlation between height and floral morphology. This may be caused by unconstrained allometries when selecting for smaller plants where resource limitation may be less stringent than when selecting for taller plants.

In contrast to flower size, we found mismatches of our predictions of the response of floral volatiles to artificial- and bumblebee-selection in the cases where predictions of reduced scent concentration were not observed. This finding is consistent with another study using the same plant genotypes and conducting bi-directional artificial selection on floral volatiles, which showed that they responded strongly to upward selection but hardly changed in response to downward selection (Zu *et al.*, 2016). This lack of response for reduced concentrations may be caused by the natural low amounts of volatiles in the starting population, minimizing the genetic variance in the downward direction (Zu *et al.*, 2016). Finally, the large overshooting of the predictions of the response of plant height and flower size in the bumblebee experiment is probably due to an overestimation of the genetic variance of the morphological traits, although we cannot test for this hypothesis because we are missing an estimate of the G-matrix in that 9-generation selection experiment.

In contrast to predictions in the bumblebee-pollinated plants, the ones in hoverfly-pollinated plants were largely not different from zero or incorrect. The observed changes were also not consistently in the same direction, implying that an evolutionary response along one major axis of overall positive trait co-variation is not likely, at least when estimating the co-linearity of the response vector with $\boldsymbol{g}_{\max}$ of $\mathbf{G}_{\text{control}}$. Instead, the observed change is more consistent with very weak selection and altered patterns of trait covariation. Indeed, in the hoverfly-selection experiment, a separate study found very little adaptive evolution in plant traits with the exception of strongly increased autonomous selfing (Gervasi & Schiestl, 2017). Thus, increased selfing and the associated reduction of genetic variation (Charlesworth, 2003), possibly altered the G-matrix, leading to the low accuracy of our predictions and the reduced efficiency of pollinator-induced selection. Previous studies in bottlenecked insect populations have shown that rapid changes in the G-matrix are expected in inbred populations (e.g., Phillips et al. 2001, Whitlock et al. 2002).

Targets of bumblebee selection

bioRxiv preprint doi: https://doi.org/10.1101/675413; this version posted June 20, 2019. The copyright holder for this preprint (which was not certified by peer review) is the author/funder. All rights reserved. No reuse allowed without permission.

Overall, bumblebee selection was in favor of taller plants with bigger petals and increased concentration of certain odor volatiles, most notably indole and methyl benzoate (see also Gervasi and Schiestl 2017). Because of the largely positive genetic correlation of most floral traits with height, it is not surprising to observe positive selection responses of those traits, and our evolutionary predictions match well with that pattern. However, our analysis revealed that some of those responses may be maladaptive because opposed to the selection gradient acting on them (e.g., benzaldehyde and benzyl nitrile, see Tables 1 and S2). This suggests that bumblebees tended to dislike flowers with increased concentration of those volatiles, whose increased observed amounts were caused by indirect selection on height and other positively correlated traits under positive selection. These indirect selection responses thus pushed the trait values further away from their optimum values and have emphasized or even created the negative selection gradient acting on them. However, without estimates of the selection gradient at each generation we cannot ascertain whether those traits are generally under negative selection by pollinators who disliked such compounds from the start or whether the negative selection gradients appeared as an indirect consequence of pollinator selection on correlated traits after the start of the selection experiment. In any case, their positive, non-adaptive responses point to the existence of strong evolutionary constraints acting on them. Overall, knowledge of the selection gradient, the G-matrix and selection response of the traits showed that they evolved in a direction biased towards $\boldsymbol{g}_{\max}$, the "line of least resistance" (Schluter 1996), which constrained the evolutionary response away from the selection gradient, although the selection responses of some traits were enhanced by trait covariation.

The role of genetic covariance in adaptive evolution

Our results are in line with the established expectation that genetic covariance can influence traits' evolutionary response by constraining or augmenting their response to selection depending on the relative signs of genetic covariances and selection gradients (Lande 1979; Arnold et al. 2001; Walsh & Blows 2009). This expectation has been rarely directly tested with experimental evolution as we did here (see also Careau et al. 2014). More commonly, empirical studies use estimates of contemporary selection gradients and G-matrices to evaluate the potential for evolutionary constraints, which are present in some cases (e.g., Blows et al. 2004; Smith &

bioRxiv preprint doi: https://doi.org/10.1101/675413; this version posted June 20, 2019. The copyright holder for this preprint (which was not certified by peer review) is the author/funder. All rights reserved. No reuse allowed without permission.

Rausher 2008; Wailing et al. 2014; Teplitsky et al. 2014) but not in others (e.g., Merilä & Björklund 1999; McGuigan et al. 2005; Berner et al. 2010).

The relevance of predictions of evolutionary constraints depends on the constancy of patterns of genetic variance-covariance over time. Our study shows that constancy cannot be assured when selection strongly reduces the genetic variance of a trait, as during artificial selection for taller plants (see also Doroszuk et al. 2008; Björklund et al. 2013; Careau et al. 2014). Yet, using $\mathbf{G}_{\text{control}}$ as an estimate of the ancestral G-matrix allowed us to make correct evolutionary predictions in most cases. Had we used $\mathbf{G}_{\text{tall}}$ in the tall selection experiment, we would have badly underestimated the selection response of plant height and floral scent (results not shown). This illustrates two important points concerning the evolutionary significance of the structure of the G-matrix. First, changes in **G** can happen quickly, over just a few generations, and we have illustrated a rapid change in trait variance caused by selection. Second, despite those changes, estimation of **G** is still useful to make predictions of future trait changes over few generations. This can be useful to predict evolution and adaptation under rapid environmental changes, for instance, because the state of the G-matrix before a change in selection pressures will strongly influence the resulting evolutionary trajectory of a population, as we have shown.

The evolutionary significance of the structure of the G-matrix is still debated, especially regarding the interpretation of the constraining effects of the main eigenvectors of **G** (especially $\boldsymbol{g}_{\text{max}}$). The debate, however, mostly crystallized on inferences of past evolutionary constraints from contemporary estimates of trait variance-covariance patterns. The retrospective use of **G** is questionable knowing how evolutionarily labile are patterns of variance-covariance, an important caveat already emphasized by Turelli (1988). Indeed, many processes may affect the evolution of trait variance and covariances because they depend on variation in allele frequencies in a population. As such, genetic drift (Jones et al. 2003) and fluctuating selection (Jones et al. 2004), have been shown to reduce the stability of the G-matrix, while migration (Guillaume & Whitlock 2007), correlational selection (Jones et al. 2003), and mutation (Jones et al. 2003, Chebib & Guillaume 2017) can improve its stability (reviewed in Arnold et al. 2008). Those changes thus make retrospective use of **G** at the least dangerous, unless its long-term stability can be determined. Prospective use of **G** is potentially less sensitive to such variations when predicting short term

bioRxiv preprint doi: https://doi.org/10.1101/675413; this version posted June 20, 2019. The copyright holder for this preprint (which was not certified by peer review) is the author/funder. All rights reserved. No reuse allowed without permission.

selection responses. Our analysis provides a good illustration of the prospective versus retrospective usage of a G-matrix when considering the changes in **G**'s structure between $\mathbf{G}_{control}$ and $\mathbf{G}_{tall}$ and the respective predictions and inferences we can make from them.

Outlook

Our study showed that even highly plastic chemical traits such as floral scent, can be successfully included into predictive models of floral trait evolution. Even more so, we show that a complementary set of traits is important to consider, because pollinator selection acts on multiple traits, and genetic correlations link them in their evolutionary response. In the future, improved sampling and analysis techniques may allow the standard inclusion of a large set of traits and large sample sizes into evolutionary studies. Larger sample sizes may allow more accurate prediction models by incorporating the dynamics of G-matrix evolution over multiple generations. In addition, more assessments of selection on those traits in nature by specific groups of interacting organisms (Ehrlén *et al.*, 2012; Ågren *et al.*, 2013; Vanhoenacker *et al.*, 2013; Gross *et al.*, 2016; Ramos & Schiestl, 2019) may further improve our ability to predict evolutionary changes in the face of environmental change in natural habitats.

Materials and methods

The workflow of the main analysis procedures is summarized in Fig. S1.

Plant species and focal traits

In our experiment, we used the rapid cycling *Brassica rapa* L. (syn. *B. campestris*: Brassicaceae) from the Wisconsin Fast Plants™ Program (Carolina Biological Supply Company, Burlington, NC, USA), selected for short generation time, rapid seed maturation, absence of seed dormancy, small plant size and high female fertility (Williams & Hill, 1986). *Brassica rapa* is a self-incompatible species with a generalized pollination system (e.g. bees, syrphid flies and butterflies as pollinators). The line used needs only ca. 35 to 40 days to complete a life cycle and maintains sufficient genetic variability for selection experiments (Miller & Schemske, 1990; Ågren & Schemske, 1992; Zu *et al.*, 2016; Zu & Schiestl, 2017).

Our analysis includes a total of 16 traits with 12 floral volatile organic compounds (VOCs), and 4 morphological traits (plant height, petal width, petal

bioRxiv preprint doi: https://doi.org/10.1101/675413; this version posted June 20, 2019. The copyright holder for this preprint (which was not certified by peer review) is the author/funder. All rights reserved. No reuse allowed without permission.

length, and flower diameter). The measurement methods were described in detail in Zu & Schiestl (2017). Floral VOCs were collected from at least four freshly opened flowers per plant at a flow rate of 100 mL per min for 3 hours. Floral VOC amounts were standardized in amounts per flower per liter sampled air, and log transformed (by ln(x +1), x being the raw value) prior to statistical analysis to approach normal distributions. Scent collection and analysis details can be found in Supporting information. The whole experiment was conducted at the Botanical Garden of the University of Zürich.

Experiment I: artificial selection experiment

Details of the experimental procedure for artificial selection can be found in Zu & Schiestl (2017). To summarize, we sowed out 150 seeds to form the parental generation. Up and down directional artificial selection on plant height were imposed to produce a tall and a short line with the ten tallest and ten shortest plants, respectively. Additionally, ten randomly selected plants were chosen to form a control line. Selected plants were randomly hand pollinated within each line. Pollen donor, pollen receiver and their offspring were labeled for each fruit to generate a breeding pedigree. After fruit maturation, around 50 seeds from each of the three lines were sown out to form the next generation. The same procedures were carried out to obtain three generations of selection. Extra seeds were sowed out to ensure a minimum of 150 individual plants in each generation. In total, we analyzed 628 plants. The experiment was conducted in a phytotron with 24h fluorescent light per day, 22°C, 60% relative humidity, and regular watering twice a day (at 08:00 and 18:00).

Experiment II: pollinator selection experiments

The procedures of experimental evolution experiment can be found in detail in Gervasi & Schiestl (2017). To summarize, we sowed out 300 seeds to generate 108 full sib families by manual cross pollination. These 108 full sib families were then equally divided into three replicates each containing 36 plants, for each of the three treatments (bumblebee, hoverfly, and hand pollination treatment). In each replicate, the 36 plants were placed in a 6×6 array with a distance of 20 cm from each other in a flight cage (2.5m×1.8m×1.2m). In bumblebee and hoverfly treatments, five pollinators (either *Bombus terrestris* or *Episyrphus balteatus*) were introduced one at a time in the flight cage, with each allowed to freely visit maximal three different

bioRxiv preprint doi: https://doi.org/10.1101/675413; this version posted June 20, 2019. The copyright holder for this preprint (which was not certified by peer review) is the author/funder. All rights reserved. No reuse allowed without permission.

plants before being removed from the cage. A total number of 12 - 15 out of 36 plants per replicate received one or more pollinator visitation. The average (± s.d.) visitation (in visited plants) was 1.35 ± 0.63 for bumblebee-pollinated plants and 1.28 ± 0.53 for hoverfly-pollinated plants. In the control treatment 12 plants were randomly chosen and were manually pollinated among each other. Floral traits were measured prior to pollinators' visits or hand pollination. The number of seeds were recorded after fruit maturation. Seeds from the pollinated plants were sown out proportionally ((individual seed set /replicate sum of seeds)×36, values below 0.5 were rounded up to 1) to form again a total number of 36 plants for the next generation of each replicate. The same selection and sowing-out procedures were conducted for 9 generations, after which plants were sowed out again and randomly hand crossed between the replicates within each treatment to get rid of potential inbreeding depression. Fruits from random crosses were sown out to form the 11th generation and the measurements of floral traits in this generation were used as observed responses to selection.

Estimation of the genetic variance-covariance matrices (G-matrix)

With known breeding pedigree and plant trait values for each individual in the control and treatment lines of the artificial selection experiment, we were able to estimate three genetic variance-covariance matrices: $\mathbf{G}_{control}$ in control, $\mathbf{G}_{tall}$ (or $\mathbf{G}_{short}$) in selection lines for increased (or decreased) plant height (see Table S3). The pedigree of the seeds sowed in the pollinator experiment was unknown. We thus used $\mathbf{G}_{control}$ from artificial selection experiment for evolutionary predictions in both experiments. More specifically, we estimated the G-matrix of the 16 traits by using a multivariate animal model in which the kinship (relatedness) matrix was obtained from the four-generation pedigree of the plants crossed within the experiments (sire = pollen donor, dam = pollen receiver), independently in the control, tall, and short experimental lines (Table S3). We fitted a linear mixed model using the Bayesian method implemented in the MCMCglmm R package (Hadfield, 2010) to estimate random effect variance components for additive genetic effects (V_A) from which we estimated the G-matrix, and among-dam (V_D) and among-sire (V_S) components to remove potential maternal and paternal effects, respectively. We added generation as a block factor modeled as a fixed effect. This method was previously shown to have good applications with a few traits (Reid, 2012; Teplitsky *et al.*, 2014).

bioRxiv preprint doi: https://doi.org/10.1101/675413; this version posted June 20, 2019. The copyright holder for this preprint (which was not certified by peer review) is the author/funder. All rights reserved. No reuse allowed without permission.

In MCMCglmm, we used weakly informative inverse-Wishart prior with limit variance of one and covariance of zero and low degree of belief (0.002). Posterior distributions were robust to several different prior settings (e.g. V = diag(n)×0.1, V = diag(n)×10, n = number of traits). We used 1,200,000 iterations, with a burn-in of 200,000 and a thinning of 500 to ensure convergence and low autocorrelation among thinned samples (< 0.1). The thinning resulted in a posterior distribution with 2000 samples.

Finally, because the Bayesian approach does not allow us to directly test for the accuracy of our estimates of the G-matrices, we implemented a permutation test in which we randomly shuffled the dam and sire of each offspring within each generation and re-estimated the G-matrix for each of 500 replicates using the same MCMCglmm procedure as before. To evaluate the accuracy of the observed G-matrices ($\mathbf{G}_{\text{control}}$, $\mathbf{G}_{\text{tall}}$, and $\mathbf{G}_{\text{short}}$), we then compared them to their randomized estimates, element by element. For each element, we computed an empirical *P*-value as: $P = (N_{random.estimates < observed.value})/500$. If the observed value was smaller than the mean of the random estimates, then (1 – *P*) was used instead of *P*. The random estimates were obtained from the posterior mode of the 500 random estimates of each G-matrix. An element of **G** (a variance or covariance term within **G**) was considered significant if its *P*-value was < 0.05. If it was not the case, then the specific element estimation did not capture its biological meaning.

Estimation of selection gradients

In the artificial selection experiment, we calculated the selection gradient on height (β_h) by using

$$\beta_h = S/V_P,$$

where V_P is the phenotypic variation of height and *S* the selection differential calculated as the difference between the mean plant height of the selected plants and all measured plants in the same generation.

bioRxiv preprint doi: https://doi.org/10.1101/675413; this version posted June 20, 2019. The copyright holder for this preprint (which was not certified by peer review) is the author/funder. All rights reserved. No reuse allowed without permission.

We calculated β_h in each generation and each selected line (table S1) and used its sum over the three generations to predict the accumulated evolutionary responses in each line.

In the pollinator selection experiments, we estimated the selection gradients following the partial correlation approach of Lande and Arnold (1983). We used generalized linear models with fitness as dependent variable and morphological and scent variable as covariates. We estimated fitness as the total number of seeds produced per plant (female fitness component) plus a male fitness component gained through pollen export. We calculated the male component as the product of "number of pollinator visits" (i.e. number of visits by pollinators to a given plant) times their respective efficiency. Pollinator efficiency is the average of the resulting number of "seeds per fruit" per single pollinator visit to a plant across all generations. Pollinator efficiency was strongly species dependent (mean ± S.D.: bumblebee: 10.57±6.34; hoverfly: 4.81±3.83; t_{267}=10.11, P<0.001). Fitness was ln(1+x) transformed before analysis to reach normality. The average per generation selection gradients (**β**) were calculated separately per treatment (bumblebee, hoverfly, and control), for all the measured generations and replicates combined (for details, see Gervasi and Schiestl 2017). Therefore, we used 9***β** to predict the total evolutionary changes after 9 generations of pollinator selection. The non-significant selection gradients were still used as the best approximate estimations of selection.

Calculation of predicted and observed evolutionary changes

To estimate the predicted responses to selection, we used the multivariate breeder's equation (Lande, 1979), $\Delta\mathbf{z} = \mathbf{G}*\boldsymbol{\beta}$. We used **G** from the control group in the artificial selection experiment ($\mathbf{G}_{control}$, Table S3, S4) for predictions as the best estimation of genetic architecture of the original population. We used the 2000 posterior samples of the G-matrix to generate a distribution of predicted trait changes from which we could evaluate the accuracy of our evolutionary prediction using its 95% highest posterior density (HPD) interval.

To calculate the observed trait changes, we did three step calculations as follows (Fig. S1). 1) We calculated the absolute phenotypic changes between the last and the first generation (Δz_obs. = $\bar{X}_{Fn}$ - $\bar{X}_{P}$, where n is 3 in artificial selection experiment, and 11 in pollinator selection experiment) for each line or each treatment,

bioRxiv preprint doi: https://doi.org/10.1101/675413; this version posted June 20, 2019. The copyright holder for this preprint (which was not certified by peer review) is the author/funder. All rights reserved. No reuse allowed without permission.

and P stands for 'parental'. 2) We estimated environmental fluctuations by using the control groups. Ideally, there should be no selection and no systematic changes of trait values in the control groups beside random fluctuations. However, traits values may have changed due to unaccounted-for selection pressures unknown to the experimenters. Therefore, we subtracted the predicted changes due to unknown selection ($\mathbf{G}^* \boldsymbol{\beta}_{\mathbf{control}} = \Delta \mathbf{z}_{_control_pred.}$) from the observed changes in control group to estimate environmental fluctuations. We calculated environmental fluctuations in both artificial- and pollinator-selection experiments. 3) We subtracted the environmental fluctuations (values in step 2) from the absolute changes (values in step 1) and used the resulting values as the observed evolutionary changes to compare with predicted changes. We present the observed and predicted changes scaled by the phenotypic standard deviation of each trait in the parental generation.

Direct and indirect selection responses

To examine the importance of trait covariance in affecting evolutionary trajectories, we separated the total selection response $\Delta\mathbf{z}$ of each trait into its direct and indirect components. The direct component of the predicted selection response is obtained by setting all genetic covariance to zero in $\mathbf{G}_{\text{control}}$, leading to the so-called **G0**-matrix (**G0**), and by multiplying **G0** by the selection vector $\boldsymbol{\beta}$. Accordingly, the direct response of trait *i* is the product $G_{ii}*\beta_i$, with G_{ii} the additive genetic variance of the trait (diagonal element of $\mathbf{G}_{\text{control}}$). The indirect component is then obtained by setting all diagonal elements of **G** to zero when computing $\mathbf{G}*\boldsymbol{\beta}$, which is equal to subtracting the direct component from the total response $\Delta\mathbf{z}$. The three predictions, from direct (**G0**), indirect (**G'**), and total response (**G**) were compared to the observed change of each trait to evaluate when the direct response is constrained (direct and indirect components of opposite sign) or enhanced (direct and indirect components of same sign) by genetic covariance.

Finally, we measured the constraining effect of genetic co-variation on the response to selection by comparing the angle $\boldsymbol{\theta}$ between the selection response vector ($\Delta\mathbf{z}$) and the first PC of **G** (PC1, or $\boldsymbol{g}_{\max}$) with the angle $\boldsymbol{\gamma}$ between $\Delta\mathbf{z}$ and the selection gradient ($\boldsymbol{\beta}$). We generated the posterior distribution of $\boldsymbol{\theta}$ from the posterior distribution of $\mathbf{G}_{\text{control}}$, which allowed us to test whether $\boldsymbol{\gamma}$ is larger (smaller) than $\boldsymbol{\theta}$, which tests if $\Delta\mathbf{z}$ is biased (unbiased) in the direction of $\boldsymbol{g}_{\max}$ by genetic correlations.

bioRxiv preprint doi: https://doi.org/10.1101/675413; this version posted June 20, 2019. The copyright holder for this preprint (which was not certified by peer review) is the author/funder. All rights reserved. No reuse allowed without permission.

G-matrices similarity among artificial selection lines

We compared the **G**-matrices from control, tall and short selection lines to assess the stability of **G** between treatments and control. We used the random skewers (RS) method in one comparison test because it examines the similarity between two **G**-matrices of their expected evolutionary response to a random set of selection vectors (skewers), which fits our purpose of evaluating the stability of such predictions using different estimates of the **G**-matrix. We used Roff et al.'s (2012) implementation of the RS method, and report the mean over 10,000 random selection skewers of the correlation between the selection response vectors of the two **G**-matrices compared. Significance was obtained from the distribution of the test statistics obtained from the 500 random estimates of each **G**-matrix. We performed a further test of shape similarity between the **G**-matrices using the hierarchical approach of Roff et al. (2012), also known as the Flury hierarchy (Phillips & Arnold, 1999). This method tests the degree of shape similarity sequentially by comparing the size and orientation of the eigenvectors (principal components, PCs) of the **G**-matrices. Two **G**-matrices can have common principal components (CPC) if their PCs have the same orientation but not the same size (i.e., have different eigenvalues), be proportional if their PCs only differ proportionally, or be equal. The three levels of similarity are tested relative to the hypothesis of unrelated matrices. The test statistics are provided in Roff et al. (2012). We determined the significance of the RS and Flury tests using the previous 500 randomized estimates of $\mathbf{G}_{control}$, $\mathbf{G}_{tall}$, and $\mathbf{G}_{short}$.

All statistics were conducted with R version 3.3.3. (R Core Team, 2017).

Acknowledgement

We thank Jarrod Hadfield for his fast and helpful reply whenever we had questions related to MCMCglmm approach. The research leading to these results has received funding from the European Union’s Seventh Framework Programme (FP7/2007-2013, FP7/2007-2011) under grant agreement no. 281093. FG was supported by grant PP00P3_144846 from the Swiss National Science Foundation.

Supporting information

bioRxiv preprint doi: https://doi.org/10.1101/675413; this version posted June 20, 2019. The copyright holder for this preprint (which was not certified by peer review) is the author/funder. All rights reserved. No reuse allowed without permission.

Details of some methods parts, *i.e.* floral scent collection and analysis, and comparing shape, size and orientation of **G**-matrices; as well as some additional supporting result tables and figures that cited in the main text can be found in the Supporting information part of this article.

Author Contribution

PZ, FS, DG performed experimental data analysis; PZ, FG performed most of the evolutionary statistical analysis; XL, DR performed part of the prediction analysis; PZ, FS, FG wrote the manuscript; all authors revised the manuscript.

References

Agrawal AA, Conner JK, Rasmann S. 2010. Tradeoffs and negative correlations in evolutionary ecology. *Evolution since Darwin: the first* **150**: 243-268.

Ågren J, Hellström F, Toräng P, Ehrlén J. 2013. Mutualists and antagonists drive among-population variation in selection and evolution of floral display in a perennial herb. *Proceedings of the National Academy of Sciences* **110**(45): 18202-18207.

Ågren J, Schemske DW. 1992. Artificial selection on trichome number in Brassica rapa. *Theoretical and Applied Genetics* **83**(6-7): 673-678.

Ashman TL, Majetic CJ. 2006. Genetic constraints on floral evolution: a review and evaluation of patterns. *Heredity* **96**(5): 343-352.

Campbell DR. 1996. Evolution of floral traits in a hermaphroditic plant: field measurements of heritabilities and genetic correlations. *Evolution* **50**(4): 1442-1453.

Caruso CM. 2004. The quantitative genetics of floral trait variation in Lobelia: potential constraints on adaptive evolution. *Evolution* **58**(4): 732-740.

Charlesworth D. 2003. Effects of inbreeding on the genetic diversity of populations. *Philosophical Transactions of the Royal Society B: Biological Sciences* **358**(1434): 1051-1070.

Darwin C. 1862. *On the various Contrivances by which British and Foreign Orchids are Fertilised by Insects*. London: John Murray.

Ehrlén J, Borg-Karlson A-K, Kolb A. 2012. Selection on plant optical traits and floral scent: Effects via seed development and antagonistic interactions. *Basic and Applied Ecology* **13**(6): 509-515.

bioRxiv preprint doi: https://doi.org/10.1101/675413; this version posted June 20, 2019. The copyright holder for this preprint (which was not certified by peer review) is the author/funder. All rights reserved. No reuse allowed without permission.

Gómez JM. 2003. Herbivory reduces the strength of pollinator-mediated selection in the Mediterranean herb Erysimum mediohispanicum: consequences for plant specialization. *The American Naturalist* **162**(2): 242-256.

Galen C. 1996. Rates of floral evolution: adaptation to bumblebee pollination in an alpine wildflower, Polemonium viscosum. *Evolution* **50**(1): 120-125.

Gervasi D, Schiestl FP. 2017. Real time divergent evolution in plants driven by pollinators. *Nature Communications* **DOI: 10.1038/ncomms14691**.

Grant V. 1949. Pollination systems as isolating mechanisms in angiosperms. *Evolution* **3**: 82-97.

Gross K, Sun M, Schiestl FP. 2016. Why do floral perfumes become different? Region-specific selection on floral scent in a terrestrial orchid. *Plos One* **11**(2): e0147975.

Hadfield JD. 2010. MCMC methods for multi-response generalized linear mixed models: the MCMCglmm R package. *Journal of Statistical Software* **33**(2): 1-22.

Hopkins R, Rausher MD. 2012. Pollinator-mediated selection on flower color allele drives reinforcement. *Science* **335**(6072): 1090-1092.

Houle D. 1992. Comparing evolvability and variability of quantitative traits. *Genetics* **130**(1): 195-204.

Irwin RE, Strauss SY. 2005. Flower color microevolution in wild radish: evolutionary response to pollinator-mediated selection. *The American Naturalist* **165**(2): 225-237.

Kaczorowski RL, Juenger TE, Holtsford TP. 2008. Heritability and correlation structure of nectar and floral morphology traits in Nicotiana alata. *Evolution* **62**(7): 1738-1750.

Lande R. 1979. Quantitative genetic analysis of multivariate evolution, applied to brain: body size allometry. *Evolution* **33**(1): 402-416.

Lande R, Arnold SJ. 1983. The measurement of selection on correlated characters. *Evolution* **37**(6): 1210-1226.

Leonard AS, Francis JS. 2017. Plant–animal communication: past, present and future. *Evolutionary Ecology* **31**(2): 143-151.

Miller TE, Schemske DW. 1990. An experimental study of competitive performance in Brassica rapa (Cruciferae). *American Journal of Botany* **77**(8): 993-998.

bioRxiv preprint doi: https://doi.org/10.1101/675413; this version posted June 20, 2019. The copyright holder for this preprint (which was not certified by peer review) is the author/funder. All rights reserved. No reuse allowed without permission.

Mitchell RJ, Shaw RG, Waser NM. 1998. Pollinator Selection, Quantitative Genetics, and Predicted Evolutionary Responses of Floral Traits in Penstemon centranthifolius (Scrophulariaceae). *International Journal of Plant Sciences* **159**(2): 331-337.

Morgan MT, Ashman TL. 2003. Quantitative character evolution under complicated sexual systems, illustrated in gynodioecious Fragaria virginiana. *The American Naturalist* **162**(2): 257-264.

Parachnowitsch AL, Raguso RA, Kessler A. 2012. Phenotypic selection to increase floral scent emission, but not flower size or colour in bee-pollinated Penstemon digitalis. *New Phytologist* **195**(3): 667-675.

R Core Team 2017. R: A language and environment for statistical computing. Vienna, Austria: R Foundation for Statistical Computing; 2017: ISBN3-900051-07-0 https://www. R-project. org.

Raguso RA, Willis MA. 2005. Synergy between visual and olfactory cues in nectar feeding by wild hawkmoths, Manduca sexta. *Animal Behaviour* **69**: 407-418.

Ramos SE, Schiestl FP. 2019. Rapid plant evolution driven by the interaction of pollination and herbivory. *Science* **364**(6436): 193-196.

Reid JM. 2012. Predicting evolutionary responses to selection on polyandry in the wild: additive genetic covariances with female extra-pair reproduction. *Proceedings of the Royal Society B Biological Sciences* **279**(1747): 4652.

Sandring S, Ågren J. 2009. Pollinator-mediated selection on floral display and flowering time in the perennial herb arabidopsis lyrata. *Evolution* **63**(5): 1292-1300.

Schiestl FP. 2015. Ecology and evolution of floral volatile-mediated information transfer in plants. *New Phytologist* **206**(2): 571-577.

Schiestl FP, Huber FK, Gomez JM. 2010. Phenotypic selection on floral scent: trade-off between attraction and deterrence? *Evol Ecol* **DOI 10.1007/s10682-010-9409-y**.

Schiestl FP, Johnson SD. 2013. Pollinator-mediated evolution of floral signals. *Trends in Ecology & Evolution* **28**(5): 307-315.

Sletvold N, Ågren J. 2010. Pollinator-mediated selection on floral display and spur length in the orchid Gymnadenia conopsea. *International Journal of Plant Sciences* **171**(9): 999-1009.

bioRxiv preprint doi: https://doi.org/10.1101/675413; this version posted June 20, 2019. The copyright holder for this preprint (which was not certified by peer review) is the author/funder. All rights reserved. No reuse allowed without permission.

Teplitsky C, Tarka M, Møller AP, Nakagawa S, Balbontín J, Burke TA, Doutrelant C, Gregoire A, Hansson B, Hasselquist D. 2014. Assessing Multivariate Constraints to Evolution across Ten Long-Term Avian Studies. *PLoS One* **9**(3): e90444.

Van Noordwijk AJ, de Jong G. 1986. Acquisition and allocation of resources: their influence on variation in life history tactics. *The American Naturalist* **128**(1): 137-142.

Vanhoenacker D, Aring, Gren J, Ehrlén J. 2013. Non-linear relationship between intensity of plant-animal interactions and selection strength. *Ecology Letters* **16**(2): 198-205.

Williams PH, Hill CB. 1986. Rapid-cycling populations of Brassica. *Science* **232**(4756): 1385-1389.

Zu P, Blanckenhorn WU, Schiestl FP. 2016. Heritability of floral volatiles and pleiotropic responses to artificial selection in Brassica rapa. *New Phytologist* **209**(3): 1208-1219.

Zu P, Schiestl FP. 2017. The effects of becoming taller: direct and pleiotropic effects of artificial selection on plant height in Brassica rapa. *The Plant Journal* **89**(5): 1009-1019.

bioRxiv preprint doi: https://doi.org/10.1101/675413; this version posted June 20, 2019. The copyright holder for this preprint (which was not certified by peer review) is the author/funder. All rights reserved. No reuse allowed without permission.

Figure Legends

Figure 1. Predicted and observed responses of various traits to artificial- and pollinator-selection (for full names of traits see Table 1). For a scaled-up version of hoverfly group see Fig. S2. The shapes of violin plots indicate the distributions of the predicted values. Black dots are the observed changes. Solid-line violin plots indicate prediction of significant evolutionary change with large confidence (95% HPD interval not overlapping with zero), whereas red and dashed-line violin plots indicate prediction of no changes (95% HPD largely overlapping with zero). Violin plots are filled when the observed changes fall within 95% HPD of predicted changes, whereas those without filling indicate the observed changes fall outside of the 95% HPD of predicted changes. Both predicted and observed changes were scaled by the phenotypic standard deviation of the trait. Sample sizes artificial selection: plant height: 600; flower size traits (PW, PL, FD): 581; volatiles: 579. Sample sizes pollinator selection: plant height: 524, flower traits: 525, volatiles: 414.

Figure 2. Comparison of the size and orientation of the major and five first eigenvectors (PCs) of the **G**-matrices in the artificial selection experiment. **a)** Distribution of the eigenvalues (size) of each PC of the three **G**-matrices in the control (grey), tall (red), and short (blue) artificial selection experiments. The scale of the *y*-axis is on the left for PC1 and on the right for PC2-5. **b)** Contribution of PC1 to the total variation in the 16 traits, measured as the size of PC1 relative to the sum of all PCs. **c)** Angle of the first and second PC with the first trait axis (height) in degree. In all cases, variation of all variables stems from the posterior distribution of each **G**-matrix estimated with MCMCglmm (see Methods and Supporting information).

bioRxiv preprint doi: https://doi.org/10.1101/675413; this version posted June 20, 2019. The copyright holder for this preprint (which was not certified by peer review) is the author/funder. All rights reserved. No reuse allowed without permission.

Table 1. Observed and predicted (total, direct and indirect) changes of traits during nine-generation selection by (A) bumblebees and (B) hoverflies. Values were scaled by the phenotypic standard deviation of the traits. Total Δz, the predicted responses from the full **G**-matrix; direct Δz, direct responses from only genetic variance (**G0**-matrix); indirect Δz, indirect responses from only genetic covariance. Δz values are given as posterior mode, the most likely estimate of a posterior distribution. Bold numbers indicate that the observed values fall within the 95% HPD of predicted changes; italic numbers indicate that the predicted changes are largely overlapping with zero.

Traits (*Abbr.*)	**Observed changes**	**Predicted changes**								
		Total			Direct			Indirect		
		Δz	95% HPD		Δz	95% HPD		Δz	95% HPD	
(A) Bumblebee										
Plant height *(Height)*	1.359	8.663	5.966	10.911	7.980	5.347	10.109	0.565	0.045	1.091
Petal width *(PW)*	0.232	1.906	0.270	3.230	0.149	0.114	0.198	**1.751**	0.130	3.072
Petal length *(PL)*	0.403	2.680	0.901	4.208	0.406	0.304	0.535	2.258	0.469	3.683
Flower diameter *(FD)*	0.241	2.071	1.132	3.617	-0.131	-0.192	-0.095	2.559	1.286	3.840

Benzaldehyde *(Ben)*	0.348	*0.710*	-1.388	3.325	-0.746	-1.011	-0.563	*1.646*	-0.582	4.208
Phenylacetaldehyde *(PAA)*	1.781	**2.071**	0.742	4.212	1.067	0.707	1.654	*1.118*	-0.407	2.711
Phenylethyl alcohol *(PhA)*	2.878	**3.848**	0.686	7.396	-0.483	-0.779	-0.367	**4.321**	1.251	8.125
Methyl salicylate *(MeS)*	-0.344	*0.886*	-1.020	2.488	-0.019	-0.026	-0.013	*0.909*	-1.003	2.507
Methyl benzoate *(MeB)*	1.031	**2.416**	0.588	4.020	**0.989**	0.706	1.329	*1.195*	-0.333	2.827
Methyl anthranilate *(MeA)*	1.221	**1.619**	0.299	3.730	-0.354	-0.504	-0.224	**2.502**	0.637	4.168
Benzyl nitrile *(BenN)*	1.729	*0.096*	-0.905	1.690	-0.694	-0.914	-0.492	*1.137*	-0.155	2.586
2-Amino benzaldehyde *(ABen)*	1.231	**1.696**	0.357	2.930	0.276	0.152	0.360	**1.411**	0.159	2.678
Indole *(Ind)*	1.238	**1.942**	0.876	3.691	0.604	0.419	0.846	**1.625**	0.357	2.952
α-Farnesene *(FAR)*	0.880	**1.951**	0.624	3.231	-0.124	-0.173	-0.099	**2.090**	0.768	3.407
Z-(3)-Hexenyl acetate *(ZHA)*	0.102	*0.999*	-0.490	2.617	-0.131	-0.174	-0.094	*1.139*	-0.336	2.773
1-Butene-4-isothiocyante *(ITC)*	0.665	*1.002*	-1.821	3.940	-0.606	-0.968	-0.395	*1.726*	-1.303	4.587
(B) Hoverfly										
Plant height *(Height)*	-0.295	2.022	1.318	2.571	1.964	1.316	2.488	*0.021*	-0.261	0.290

bioRxiv preprint doi: https://doi.org/10.1101/675413; this version posted June 20, 2019. The copyright holder for this preprint (which was not certified by peer review) is the author/funder. All rights reserved. No reuse allowed without permission.

Petal width *(PW)*	0.118	***0.354***	-0.144	0.784	-0.195	-0.260	-0.149	**0.668**	0.074	1.046
Petal length *(PL)*	0.371	**0.697**	0.246	1.145	0.094	0.071	0.124	**0.605**	0.113	0.990
Flower diameter *(FD)*	0.213	0.711	0.406	1.107	0.299	0.216	0.437	**0.389**	0.123	0.718
Benzaldehyde *(Ben)*	0.618	*-0.096*	-0.645	0.480	-0.322	-0.436	-0.243	***0.267***	-0.315	0.840
Phenylacetaldehyde *(PAA)*	0.408	*0.152*	-0.325	0.497	-0.358	-0.555	-0.237	**0.461**	0.034	0.911
Phenylethyl alcohol *(PhA)*	0.465	***0.395***	-0.440	1.119	-0.057	-0.092	-0.044	***0.372***	-0.371	1.191
Methyl salicylate *(MeS)*	-0.984	*0.012*	-0.352	0.498	0.177	0.121	0.247	*-0.074*	-0.531	0.321
Methyl benzoate *(MeB)*	0.764	*-0.001*	-0.409	0.424	-0.157	-0.210	-0.112	*0.032*	-0.250	0.592
Methyl anthranilate *((MeA)*	0.320	*-0.057*	-0.487	0.324	-0.517	-0.736	-0.328	**0.533**	0.081	0.934
Benzyl nitrile *(BenN)*	0.622	*0.183*	-0.118	0.503	0.211	0.149	0.277	*-0.042*	-0.345	0.291
2-Amino benzaldehyde *(ABen)*	0.002	***0.233***	-0.119	0.483	-0.046	-0.060	-0.025	***0.202***	-0.078	0.527
Indole *(Ind)*	0.080	0.462	0.093	0.764	0.253	0.175	0.354	***0.243***	-0.139	0.496
α-Farnesene *(FAR)*	0.767	0.512	0.207	0.863	0.228	0.182	0.318	*0.234*	-0.015	0.576
Z-(3)-Hexenyl acetate *(ZHA)*	-0.773	*-0.036*	-0.438	0.292	-0.286	-0.378	-0.204	*0.162*	-0.139	0.600

bioRxiv preprint doi: https://doi.org/10.1101/675413; this version posted June 20, 2019. The copyright holder for this preprint (which was not certified by peer review) is the author/funder. All rights reserved. No reuse allowed without permission.

1-Butene-4-isothiocyante *(ITC)*	0.868	*0.361*	-0.544	0.876	-0.013	-0.020	-0.008	*0.378*	-0.544	0.876

696

bioRxiv preprint doi: https://doi.org/10.1101/675413; this version posted June 20, 2019. The copyright holder for this preprint (which was not certified by peer review) is the author/funder. All rights reserved. No reuse allowed without permission.

bioRxiv preprint doi: https://doi.org/10.1101/675413; this version posted June 20, 2019. The copyright holder for this preprint (which was not certified by peer review) is the author/funder. All rights reserved. No reuse allowed without permission.

Table 2. Comparisons of the three G-matrices using random skewers and hierarchical analyses (see also Table S3, S4). The random skewers section reports the mean correlation among response vectors of two **G**-matrices subject to the same set of 10,000 random selection vectors. The hierarchical analysis reports the *P*-values to reject the hypotheses of equality, proportionality, or common principal components (CPC) in favor of *unrelated* matrices. The *P*-values are obtained by randomization (see Methods).

	Random Skewers		**Hierarchical**		
Paired G	**Mean correlation**	***P*-value**	**Equal**	**Prop.**	**CPC**
$\mathbf{G}_{control}$ - $\mathbf{G}_{tall}$	0.734	< 0.01[a]	< 0.005	< 0.005	0.002
$\mathbf{G}_{control}$ - $\mathbf{G}_{short}$	0. 987	< 0.002[b]	0.23	0.23	0.32
$\mathbf{G}_{tall}$ - $\mathbf{G}_{short}$	0.722	< 0.21[a]	0.19	0.19	< 0.05

[a]: left tail; [b]: right tail

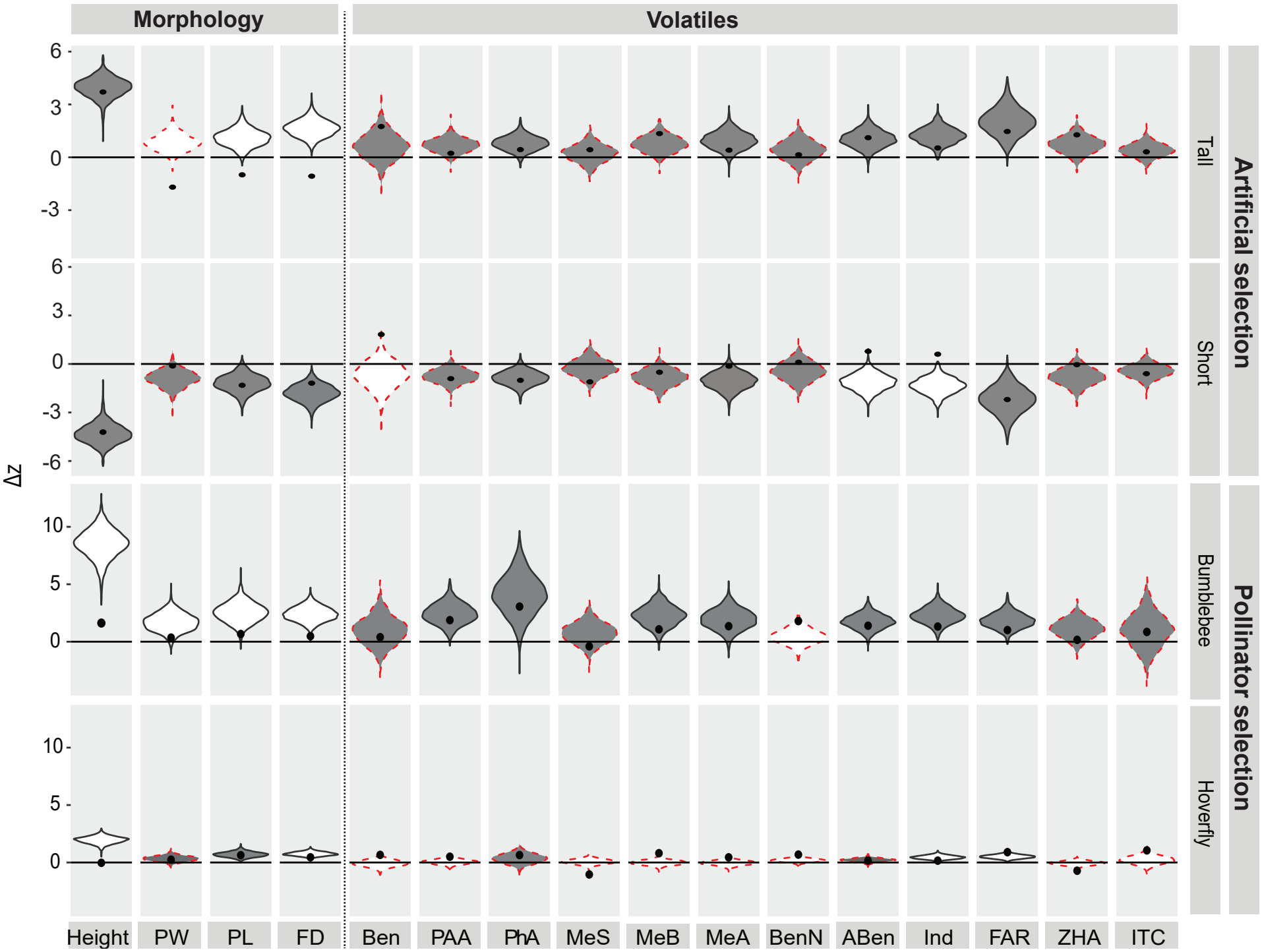
Morphology
Volatiles
Δz
Tall
Short
Bumblebee
Hoverfly
Artificial selection
Pollinator selection
Height
PW
PL
FD
Ben
PAA
PhA
MeS
MeB
MeA
BenN
ABen
Ind
FAR
ZHA
ITC

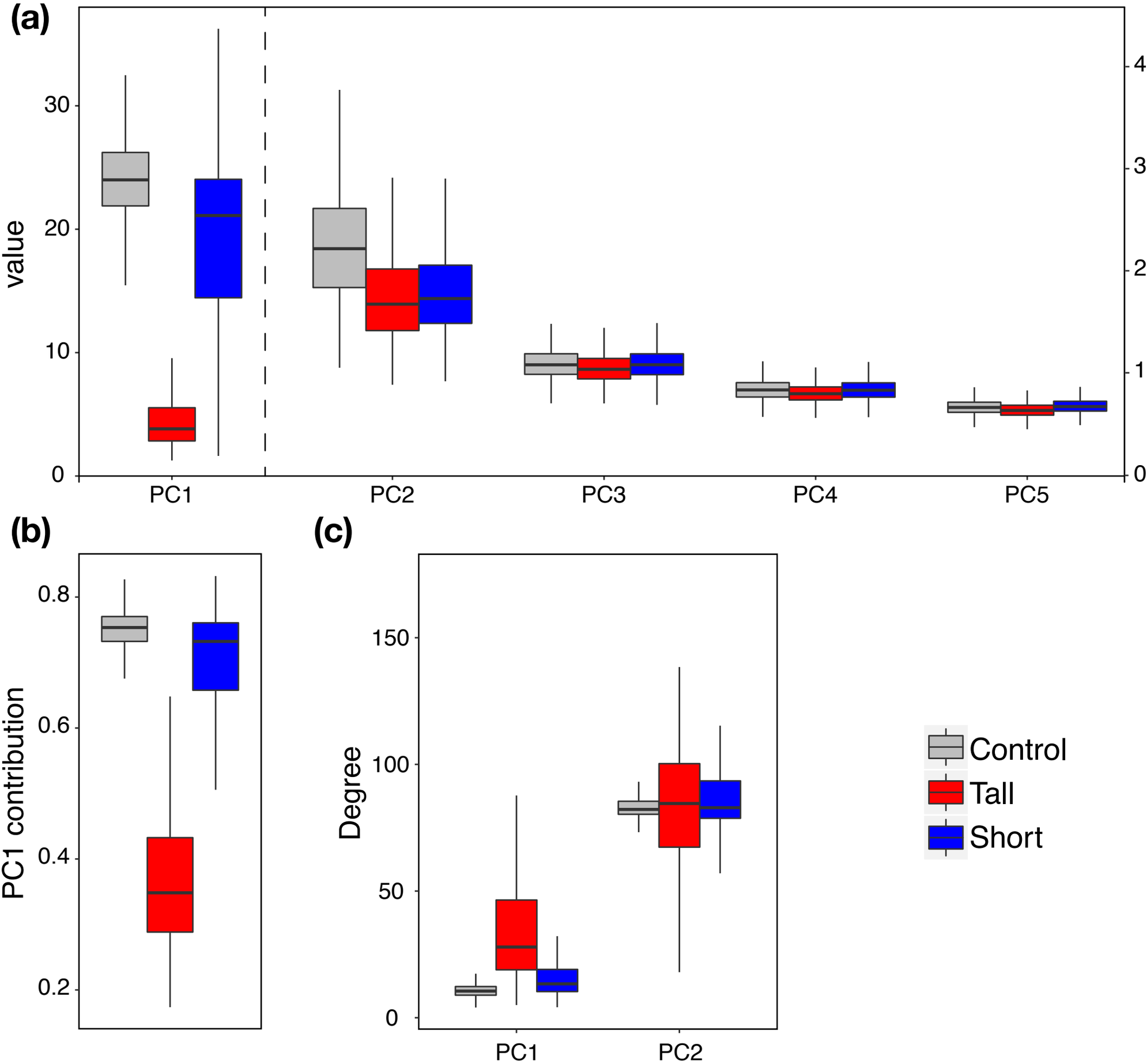
(a)
value
30
20
10
0
4
3
2
1
0
PC1
PC2
PC3
PC4
PC5
(b)
PC1 contribution
0.8
0.6
0.4
0.2
(c)
Degree
150
100
50
0
PC1
PC2
Control
Tall
Short